Electron Trapping Variations in Single-Crystal Pixelated HgI_2 Gamma-Ray Spectrometers

J. E. Baciak, *Student Member, IEEE*, Z. He, *Senior Member, IEEE*, and R. P. DeVito, *Member, IEEE*

***Abstract*—The characteristics of thick ($\sim$ 6 mm) HgI_2 room-temperature gamma-ray detectors having 4 small pixel anodes are investigated. Spectra for the different anodes (overall and for individual interaction depths) are presented. The mu–tau product for electrons was measured to study the variations of electron transport within a single HgI_2 crystal. By using the single polarity charge sensing with depth sensing, the $\mu_e\tau_e$ was estimated to vary from $\sim 9 \times 10^{-4}$ cm^2/V to 7×10^{-3} cm^2/V. Individual pixels have the ability to produce spectra with resolutions less than 3% at 662 keV. Some effects of electron detrapping and hole transport are also discussed.**

I. Introduction

SINCE the early 1970s [1], mercuric iodide (HgI_2) has been investigated as a gamma-ray spectrometer that can operate at room temperature. However, like most room-temperature semiconductor γ-ray spectrometer materials, HgI_2 suffers from poor charge transportation characteristics. Despite the fact that HgI_2 has a wide bandgap, high atomic numbers, and a high density which should lend itself to room-temperature spectroscopy applications, the crystals suffer from low electron and hole mobility, significant hole trapping, and material nonuniformity. Thus, HgI_2 detectors have been limited to uses with thin crystals ($<$ 3 mm thick) and long shaping times in order to achieve reasonable spectroscopic results.

To improve the spectroscopic performance of thicker HgI_2 detectors, one must reduce the depth dependence of the generated pulse from a γ-ray interaction event that is seen with these detectors. The use of single polarity charge sensing was implemented in order to overcome the severe hole trapping present in wide bandgap semiconductor detectors, including HgI_2. The introduction of pixelated anodes to CdZnTe [2] and HgI_2 [3] showed that one can improve the resolution of wide bandgap semiconductor detectors dramatically over the standard planar electrode configuration. By also measuring a signal from the planar cathode, which is essentially linearly dependent with the γ-ray interaction depth [4], the interaction location and energy deposition can be obtained by the cathode/anode ratio signal and the pixel anode amplitude.

In this paper, we present the latest results for HgI_2 detectors using single-polarity charge sensing and pixelated anodes with three-dimensional (3-D) position sensing. This allowed us to study the effects of spatially dependent differences in electron transportation properties and material nonuniformity of the detectors. Two main characteristics are reported. First, the raw and depth-corrected spectral resolutions are reported for each pixel at 662 keV. Then, using different cathode biases, the $\mu_e\tau_e$ is estimated using a Cs-137 source as well as an Am-241 source and the results are compared.

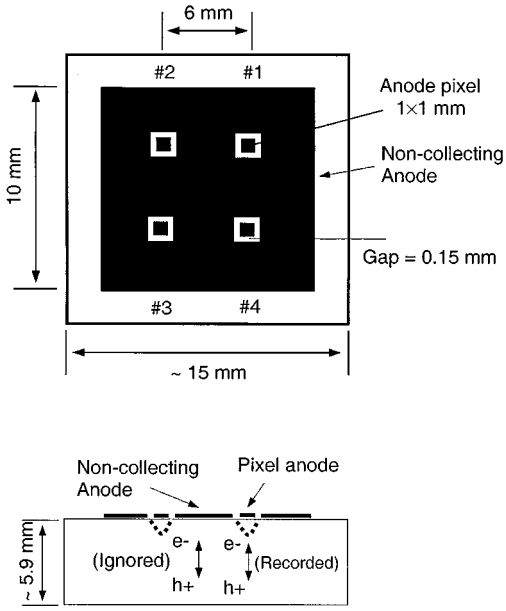

Fig. 1. Configuration for detector #92 512Q92. Top: top view of the detector and the anode configuration. Bottom: side view of the detector.

II. Detector Description

The anode pixel configuration is shown in Fig. 1. The four small pixels are surrounded on all sides by a large anode plate. The area of each pixel is $\sim$ 1 mm^2 and is comprised of Pd. Only electrons move toward the anode surface and thus the induced charge on a pixel is determined mainly by the movement and collection of electrons underneath the vicinity of each pixel. The signal produced by the anode pixel is only slightly dependent upon the distance traveled by the electrons and is not significantly affected by hole movement under the anode.

The detector electrodes are connected to AmpTek[1] A250 charge sensitive preamplifiers, which are then connected to

Manuscript received November 5, 2001. This work was supported in part by NASA STTR under Contract NAS5 00205 and Constellation Technology.

J. E. Baciak and Z. He are with the Department of Nuclear Engineering and Radiological Sciences, University of Michigan, Ann Arbor, MI 48109 USA (e-mail: jimbar@umich.edu; hezhong@umich.edu).

R. P. Devito is with Constellation Technology Corporation, Largo, FL 33777 USA (e-mail: devito@contech.com).

Publisher Item Identifier S 0018-9499(02)06155-5.

[1]Amptek, Inc., Bedford, MA 01730 USA.

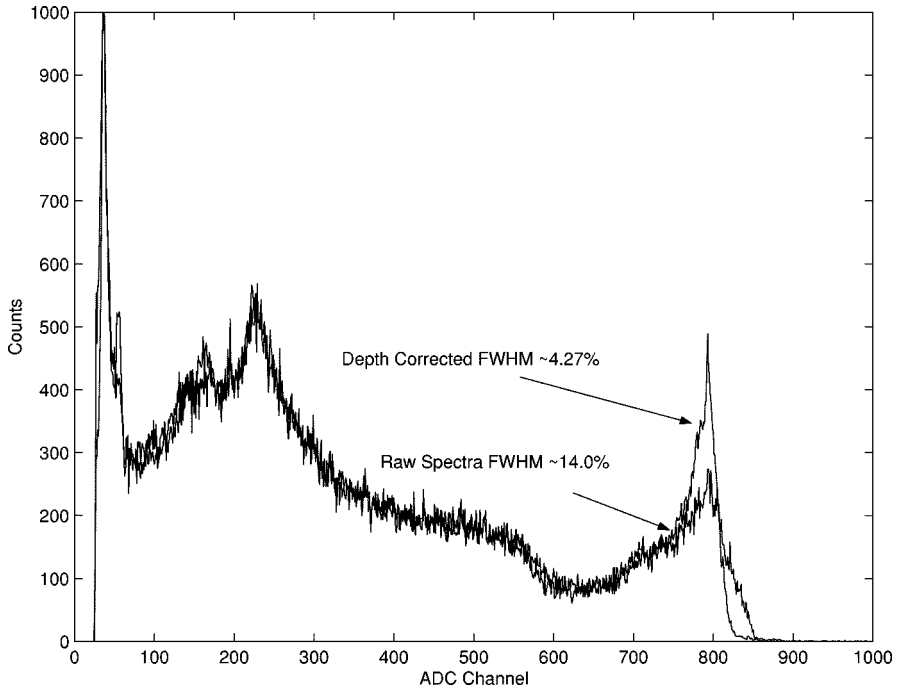

Fig. 2. Best Cs-137 spectra obtained for pixel #1. The detector bias was −2000 V and the cathode and anode shaping times were both set at 8 μs.

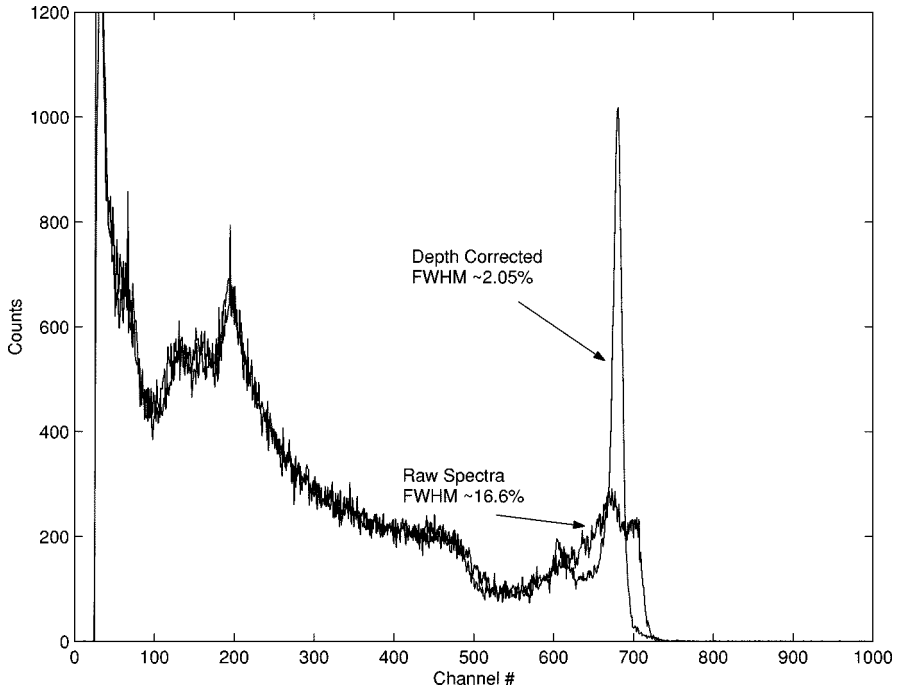

Fig. 3. Best Cs-137 spectra obtained for pixel #2. The detector bias was −1500 V, the cathode shaping time was 4 μs, and the anode shaping time was 8 μs.

shaping amplifiers for pulse shaping and amplification purposes. The signals are then fed into peak-hold circuitry to hold the peak of the shaped pulse for a sufficiently long time before the ADC samples the pulse amplitude.

III. Results and Discussion

Below, we present results for detector resolution for a Cs-137 point source and estimates for $\mu_e\tau_e$. Cs-137 spectra were collected in 22 h and Am-241 spectra were collected in 2 h.

A. Detector Resolution

Figs. 2–5 show the best obtained spectra for each individual pixel from HgI_2 detector #92 512Q92. While the resolution for the raw spectra is quite poor, there is a vast improvement once a correction for interaction depth has been performed. As can be seen, two pixels (#2 and #3) have the best resolution with 2.05% and 2.58%, respectively. pixel #1's resolution was the worst of the four pixels. While pixel #3 had good resolution, the number of counts within the Compton continuum was much larger than that of the other three pixels. Table I gives the overall raw and

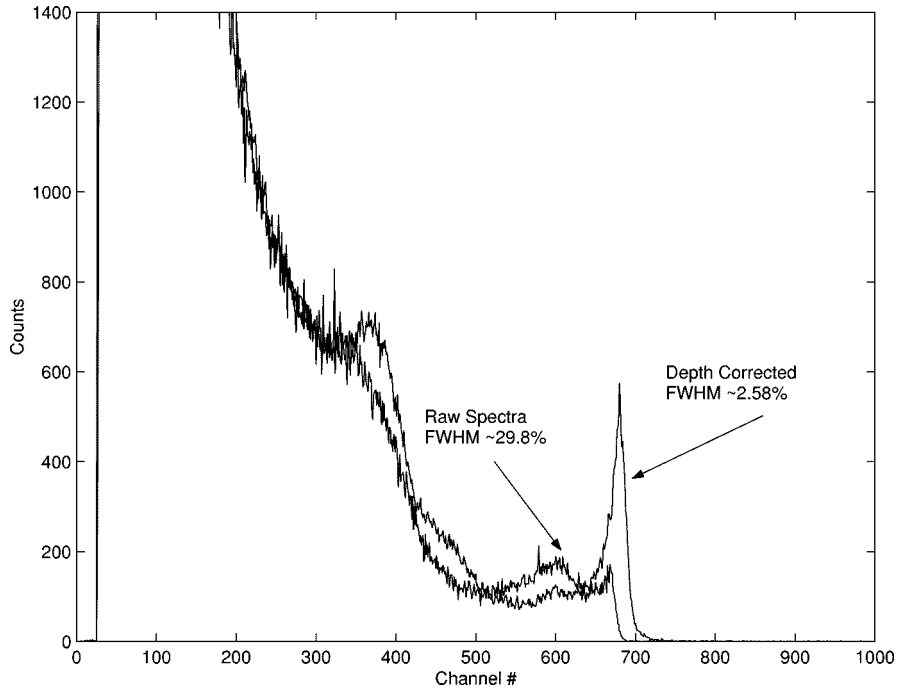

Fig. 4. Best Cs-137 spectra obtained for pixel #3. The detector bias was −1500 V and the cathode and anode shaping times were both set at 8 μs.

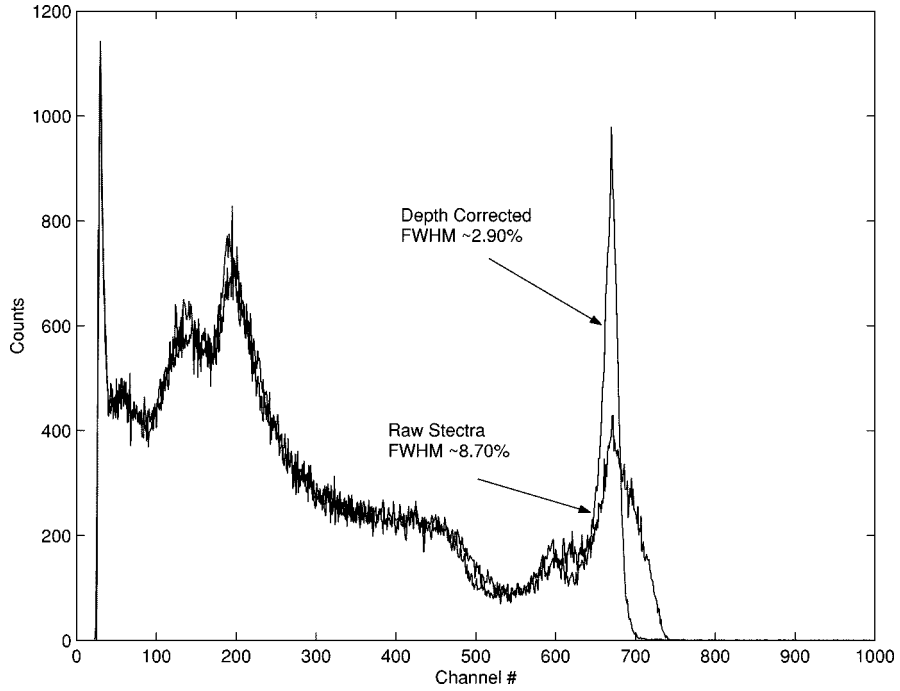

Fig. 5. Best Cs-137 spectra obtained for pixel #4. The detector bias was −1500 V and the cathode and anode shaping times were both set at 8 μs.

depth-corrected resolution for each pixel and various anode and cathode shaping time combinations.

For pixel #1, we cannot resolve the peak using depth correction to any better than a fraction over 4%. Further investigation of the resolution as a function of depth index for this pixel reveals that the resolution is quite poor for many of the depth indices (Fig. 6). While the resolution is quite decent for relatively low-valued depth indices, beginning at around Depth Index 10 the resolution becomes much worse. This sudden degradation in peak resolution could be due to degraded electron transportation under this pixel somewhere in the middle of detector. This could be caused by, to name a few, a small void in the crystal, or a grain boundary. Thus, depth correcting for the photopeak cannot vastly improve the resolution of the pixel if the resolution of individual depth indices is poor. When investigating the best pixel (pixel #2), the resolution at individual depths is very good, with resolution less than 2% for many different depths (Fig. 7). This reveals that the material and electron transportation characteristics under pixel #2 (and likewise pixel #4) are very good for single polarity charge sensing.

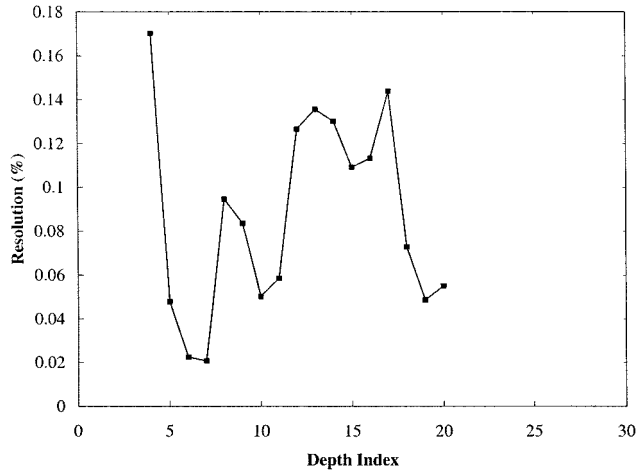

Fig. 6. Cs-137 spectral resolution for pixel #1 as a function of depth index.

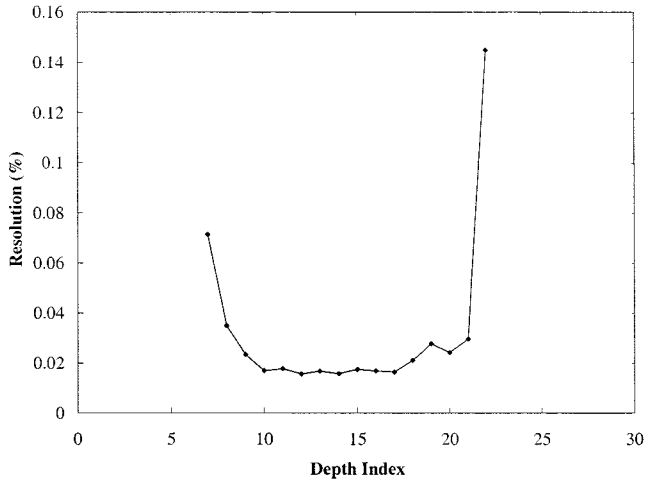

Fig. 7. Cs-137 spectral resolution for pixel #2 as a function of depth index.

TABLE I
CS-137 RESOLUTION OF THE ANODE PIXELS FOR DIFFERENT SHAPING TIME CONFIGURATIONS

Pix #1

Anode Shaping Time (μs)	Cathode Shaping Time (μs)	1500 V (raw)	1500 V (d.c.)	2000 V (raw)	2000 V (d.c.)
2	2	0.1654	0.0979	0.1643	0.0685
4	2	0.1381	0.0568	0.1486	0.441
4	4	0.156	0.0541	0.1382	0.454
8	2	0.1378	0.0414	0.143	0.0463
8	4	0.1646	0.0501	0.149	0.0466
8	8	0.1892	0.0419	0.14	0.0427

Pix#2

Anode Shaping Time (μs)	Cathode Shaping Time (μs)	1500 V (raw)	1500 V (d.c.)	2000 V (raw)	2000 V (d.c.)
2	2	0.0378	0.0316	0.0431	0.0375
4	2	0.153	0.0208	0.136	0.0213
4	4	0.125	0.0258	0.135	0.0226
8	2	0.157	0.0205	0.156	0.0221
8	4	0.166	0.0205	0.164	0.0218
8	8	0.189	0.0208	0.122	0.0254

Pix #3

Anode Shaping Time (μs)	Cathode Shaping Time (μs)	1500 V (raw)	1500 V (d.c.)	2000 V (raw)	2000 V (d.c.)
2	2	0.0499	0.0378	0.0525	0.0374
4	2	0.231	0.0346	0.213	0.0334
4	4	0.191	0.0337	0.263	0.0328
8	2	0.282	0.0348	0.202	0.0427
8	4	0.286	0.0291	0.273	0.0369
8	8	0.298	0.0258	ERROR	0.0381

Pix#4

Anode Shaping Time (μs)	Cathode Shaping Time (μs)	1500 V (raw)	1500 V (d.c.)	2000 V (raw)	2000 V (d.c.)
2	2	0.0518	0.0379	0.045	0.0366
4	2	0.0433	0.0396	0.0507	0.0361
4	4	0.0443	0.0327	0.059	0.0377
8	2	0.0797	0.0314	0.106	0.0355
8	4	0.0869	0.0316	0.1121	0.0336
8	8	0.087	0.029	0.117	0.0309

As mentioned earlier, pixel #3's Compton Continuum counts were much higher than those of the other three pixels of this detector. This may indicate that the electron collection process of this anode pixel is not ideal. The effective volume of the pixel could be smaller than normal, causing some of the electrons in the cloud to not be collected by the pixel, thereby reducing the amount of induced charge on the anode by an amount suitable to place an event in the Compton region. Investigation of the anode surface reveals that there is some degradation of the surface of this pixel. This could also severely hinder proper electron collection and cause spectra to have an unusually high Compton continuum.

Examination of Table I reveals some peculiar results. First, as the shaping time increased, the raw spectra peak resolution became slightly worse. This can partially be explained by the fact that, as the shaping time increased, the effect of hole movement can be significant, particularly for events near the cathode where holes only need to move a small fraction of the detector thickness to be collected. This will particularly increase the induced charge by interactions near the cathode. Detrapped electrons can also contribute more to the induced signal at longer shaping times and this effect will be greater for interactions near the cathode as well. Also, the depth corrected resolutions are in many cases better for the lower bias. One would expect the resolution to be better at higher biases due to more efficient charge transportation and collection. One main factor in the depth correction process is the ability to initially separate the interactions by depth according to the cathode/anode ratio. At higher detector biases and longer shaping times, hole movement can become significant, particularly for events near the cathode. While hole movement has very little effect on the anode pixel signal, it has a significant effect on the cathode signal because longer shaping times and higher detector biases allow holes to be collected by the cathode more efficiently. Events further away from the cathode will then be processed as a near cathode events. This will increase the number of counts corresponding to near cathode events. This effect can be seen in Fig. 8, whereby the 2000-V peak counts has increased significantly for events near the cathode. Therefore, better transport of holes can potentially degrade the ability to separate for interaction depth. One potential way to reduce this effect is to separate the spectra into finer depths (that is, increase the number of depth indices).

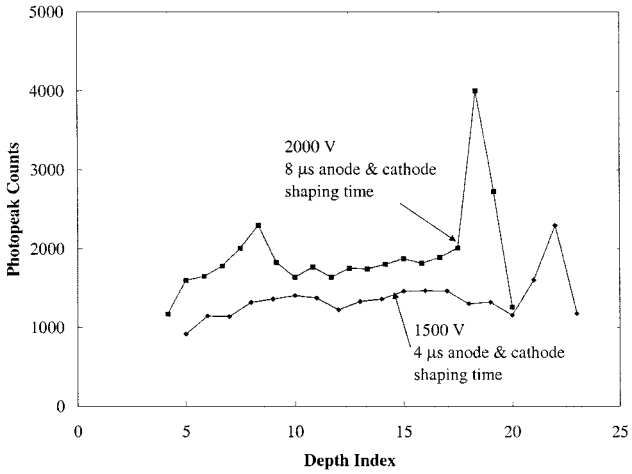

Fig. 8. Cs-137 peak counts as a function of depth index. Notice the increase in counts near the cathode as bias and shaping time are increased.

TABLE II
$\mu_e\tau_e$ ESTIMATIONS USING CS-137

Anode Shaping Time (μs)	Cathode Shaping Time (μs)	Pix #1 μτ (cm^2/V)	Pix #2 μτ (cm^2/V)	Pix #3 μτ (cm^2/V)	Pix #4 μτ (cm^2/V)
2	2	ERROR	0.00128	0.00385	0.00775
4	2	0.00090	ERROR	0.00614	0.00156
4	4	0.00133	0.00666	0.00342	0.00332
8	2	0.00193	0.00508	0.00480	0.00253
8	4	0.00163	0.00705	0.00483	0.00352
8	8	0.00515	0.00357	0.00379	0.00354

B. $\mu_e\tau_e$ Estimation

The method used to estimate the $\mu\tau$ product for electrons is described in [5]. By varying the detector bias, the amount of trapping will vary due to changes in the magnitude of the electric field within the detector. This will show up in spectra as a shift in the photopeak amplitude. This shift in photopeak amplitude is then used to estimate $\mu_e\tau_e$. The method was used at several different shaping times to investigate the effect shaping time has on the calculation.

Two different methods were used to indicate the depth index that corresponds to the photoelectric interactions nearest the cathode. In the first method, the $\mu_e\tau_e$ was calculated using a Cs-137 source. The depth index that had the highest number of peak counts was considered the cathode side, since we irradiated the detector from the cathode side. The estimated values for $\mu_e\tau_e$ using this method are shown in Table II. The $\mu_e\tau_e$ estimation can vary by almost an order of magnitude, from 9×10^{-4} cm^2/V to 7×10^{-3} cm^2/V. Pixel #2 generally had the highest values, while pixel #1 had the lowest values. Two of the values for $\mu_e\tau_e$ could not be estimated since either the peak positions at both biases were the same, or the peak position at the lower bias was higher than the one corresponding to the higher bias. It is interesting to note that the pixels that have the higher $\mu_e\tau_e$ also have better energy resolution. Thus, a correlation between electron transport properties and energy resolution can clearly be seen in this detector.

In the second method, a low-energy source was used to irradiate the detector from the cathode side, in this case Am 241.

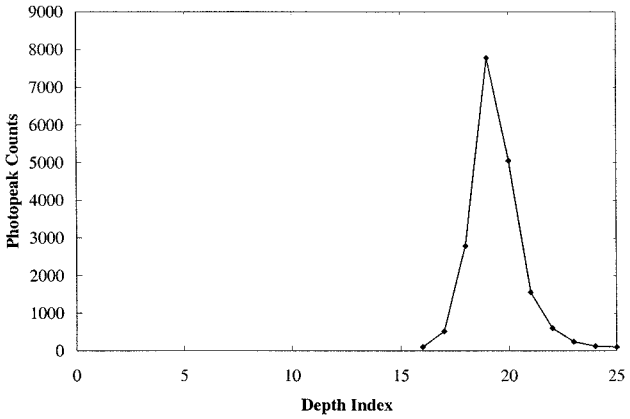

Fig. 9. Am-241 peak counts as a function of depth index for pixel #2. Notice that most of the peak counts are contained within 4 depth indices.

Greater than 90% of the 59.5-keV γ-rays emitted by Am-241 are absorbed within 0.7 mm of HgI_2. Thus most of the events in the overall spectra should also be contained in a depth index corresponding to the cathode side. This is the case as most photopeak events are contained within 3–4 depth indices (Fig. 9). Performing the same analysis on two pixels (Pixels #2 and #4) using the Am-241 source, the estimated $\mu_e\tau_e$ for Pixel #2 ranged from ~ 2.8–3.1×10^{-3} cm^2/V, from ~ 1.5–2.4×10^{-3} cm^2/V for Pixel #3 and from ~ 1.6–3.0×10^{-3} cm^2/V for Pixel #4. Similar calculations were attempted for the other pixel of detector #92 512Q92, but the values varied dramatically or could not be calculated for reasons similar to above for Cs 137. The fact that the values for $\mu_e\tau_e$ obtained using either high or low energy γ-rays were on the same order of magnitude was encouraging and shows that the $\mu_e\tau_e$ can be estimated using high energy γ-rays when operating pixelated single polarity semiconductor detectors at room temperature.

As mentioned earlier, an increase in detector bias can increase the thickness that corresponds to near cathode interactions. This increase in thickness will cause errors in the calculation since the thickness of the depth index is different for the two voltages. This effect must be eventually accounted for and corrected to increase the accuracy of the calculation for $\mu_e\tau_e$.

IV. SUMMARY

HgI_2 detectors operating via single polarity charge sensing have been tested for use as a room temperature γ-ray spectrometer and the variations in electron transport characteristics have been analyzed. The detector was designed with four small pixels within the central region of the detector surrounded by a large anode in order to take advantage of the small pixel effect. The pixel anode signal is mainly determined from electron movement within the detector and is not sensitive to the depth of the γ-ray interaction. By simultaneously measuring the cathode signal, assumed to have a linear dependence with interaction depth, the depth of the interaction can be determined by calculating the cathode/anode signal ratio and spectra can be collected as a function of interaction location.

Spectra were obtained and analyzed at two different biases and several different shaping time configurations. By using pix-

elated anodes, the resolution for three of the four pixels was less than 4% at 662 keV, with the best pixel yielding a resolution of 2.05%. At longer shaping times, electron detrapping and hole movement can also have an effect on the collected spectra and could potentially worsen the resolution. The $\mu_e\tau_e$ product was then calculated by comparing the peak centroids obtained from each pixel at different cathode biases. Only spectra obtained from near cathode γ-ray interaction events were used to calculate the $\mu_e\tau_e$. The values ranged from approximately 9×10^{-4} cm^2/V to 7×10^{-3} cm^2/V, which are higher than most published values for $\mu_e\tau_e$. These values may represent an improvement in the electron transportation properties in HgI_2. The technique used can reduce the amount of systematic errors present in other techniques. Two different sources were used, namely Am-241 and Cs-137, and the calculated $\mu_e\tau_e$ from each source is consistent with the other. This shows that this technique can be used for both low- and high-energy γ-rays. By showing that the resolution of thick HgI_2 detectors is capable of being $< 3\%$ with today's crystals, we expect that progressing to thicker devices (10 mm thick) and moving toward a fully pixelated anode along with improvements in the data acquisition system could yield better resolution from single pixel events and allow us to study multiple interaction events.

ACKNOWLEDGMENT

The authors thank Constellation Technology for the fabrication of the detector crystals.

REFERENCES

[1] W. R. Willig, "Mercury iodide as a gamma spectrometer," *Nucl. Instr. Meth.*, vol. 96, pp. 615–616, 1971.

[2] Z. He, W. Li, G. F. Knoll, D. K. Wehe, J. Berry, and C. M. Stahle, "3-D position sensitive CdZnTe gamma-ray spectrometers," *Nucl. Instr. Meth.*, vol. A422, pp. 173–178, 1999.

[3] Z. He and R. D. Vigil, "Investigation of pixellated HGI_2 γ-ray spectrometers," *Nucl. Instr. Meth.*, pt. A, 2002.

[4] Z. He, G. F. Knoll, D. K. Wehe, R. Rojeski, C. H. Mastrangelo, M. Hammig, C. Barrett, and A. Uritani, "1-D position sensitive single carrier semiconductor detectors," *Nucl. Instr. Meth.*, vol. A380, pp. 228–231, 1996.

[5] Z. He, G. F. Knoll, and D. K. Wehe, "Direct measurement of $\mu_e\tau_e$ of CdZnTe semiconductors using position sensitive charge sensing detectors," *J. App. Phys.*, vol. 84, no. 10, pp. 5566–5569, 1998.